END
DATE
FILMED

5 -82

DTIC

MICROCOPY RESOLUTION TEST CHART
NATIONAL BUREAU

⑫

CORROSION LABORATORY
MASSACHUSETTS INSTITUTE OF TECHNOLOGY

HYDROGEN INDUCED INTERGRANULAR CRACKING

OF NICKEL-BASE ALLOYS

By

R.M. Latanision

Final Technical Report

to

Office of Naval Research

Contract No. N00014-78-C-0002, NR 036-127/8-24-77(471)

Reproduction in whole or in part is
permitted for any purpose of the
United States Government

Corrosion Laboratory
Department of Materials Science and Engineering
Massachusetts Institute of Technology
Cambridge, Massachusetts 02139

February 1982

SECURITY CLASSIFICATION OF THIS PAGE (When Data Entered)

REPORT DOCUMENTATION PAGE		READ INSTRUCTIONS BEFORE COMPLETING FORM
1. REPORT NUMBER	2. GOVT ACCESSION NO. AD-A113 425	3. RECIPIENT'S CATALOG NUMBER
4. TITLE (and Subtitle) Hydrogen Induced Intergranular Cracking of Nickel-Base Alloys		5. TYPE OF REPORT & PERIOD COVERED Final Technical Report
		6. PERFORMING ORG. REPORT NUMBER
7. AUTHOR(s) R.M. Latanision		8. CONTRACT OR GRANT NUMBER(s) N00014-78-C-0002 NR036-127/8-24-77(471)
9. PERFORMING ORGANIZATION NAME AND ADDRESS Massachusetts Institute of Technology Cambridge, Massachusetts 02139		10. PROGRAM ELEMENT, PROJECT, TASK AREA & WORK UNIT NUMBERS
11. CONTROLLING OFFICE NAME AND ADDRESS Office of Naval Research 800 Quincy Street Arlington, Virginia 22217		12. REPORT DATE February 1982
		13. NUMBER OF PAGES 14
14. MONITORING AGENCY NAME & ADDRESS(if different from Controlling Office)		15. SECURITY CLASS. (of this report)
		15a. DECLASSIFICATION/DOWNGRADING SCHEDULE

16. DISTRIBUTION STATEMENT (of this Report)

DISTRIBUTION STATEMENT A
Approved for public release;
Distribution Unlimited

17. DISTRIBUTION STATEMENT (of the abstract entered in Block 20, if different from Report)

18. SUPPLEMENTARY NOTES

19. KEY WORDS (Continue on reverse side if necessary and identify by block number)

hydrogen permeation, hydrogen embrittlement, nickel-base al,
hydrogen transport processes, solute segregation.

20. ABSTRACT (Continue on reverse side if necessary and identify by block number)

This final report is intended to summarize the activities pursued during the course of a program directed toward an evaluation of the susceptibility of nickel and nickel-base alloys to embrittlement by cathodically produced hydrogen. The transport of hydrogen by lattice and grain boundary diffusion, as well as by mobile dislocations, has been examined.

DD FORM 1473 EDITION OF 1 NOV 65 IS OBSOLETE
1 JAN 73
S/N 0102-LF-014-6601

Introduction

It is well known that the absorption of hydrogen, whether introduced by electrochemical or gas phase charging, leads to the intergranular embrittlement of polycrystalline nickel and some nickel-base alloys (see Ref. 1 for a general review). It is also observed that intergranular separation occurs over distances in bulk specimens that are far larger than the depth of penetration expected from lattice diffusion of hydrogen: for example, the full cross section of 2 mm diameter specimens strained in tension at $\dot{\epsilon} \approx 10^{-4}$ sec^{-1} and cathodically charged with hydrogen at 25°C has been observed to intergranularly embrittle in a matter of minutes (2). There is, however, evidence to suggest that grain boundary segregates (particularly metalloid impurities) may play a role in hydrogen absorption at grain boundaries as first proposed by Latanision and Opperhauser (2). At the inception of this program, however, there was little, if any, direct evidence to suggest short circuiting diffusion via grain boundaries, dislocation pipes or rapid transport of hydrogen by other means that might account for the observed extent and degree of embrittlement. On the other hand, serrated yielding has been observed in nickel single crystals which were simultaneously charged with hydrogen and deformed in tension <u>at ambient temperatures</u> (3). The latter is an indication of (mobile) dislocation - solute (hydrogen) interactions and suggested the possibility that dislocation transport of hydrogen may be involved in the embrittlement process.

Direction and Results of This Program

Given the above, research proceeded along two principal directions in this program: Firstly, electrochemical hydrogen permeation experiments were conducted on specimens of polycrystalline nickel and nickel-base alloys in order to investigate whether the transport of hydrogen by mobile dislocations may have contributed to the ingress of hydrogen during experiments such as those described earlier. Secondly, we wished to examine, by both electrochemical permeation techniques and ion-microprobe analysis, the possibility that grain boundary transport might occur during cathodic charging.

The results of these studies have been described in earlier technical reports and publications. Kurkela (4,5) has observed transport rates far in excess of lattice diffusion in his work on specimens of nickel and nickel-base alloys undergoing plastic deformation during cathodic charging. The effects of strain rate, grain size, coherent precipitates, and other metallurgical parameters on permeation transient behavior are compatible with dislocation transport of hydrogen in the form of core atmospheres. It must be mentioned that concern has been expressed by Otsuka and Isaji (6) that some aspects of the transient behavior on nickel specimens undergoing plastic deformation may arise from Joule heating effects. While there can be no doubt that Joule heating may occur when a current passes through a conductor (whether metal electrode, electrolyte or at the metal-electrolyte interface), we consider that much of the phenomenology that has been observed on straining membranes is best understood in terms of hydrogen permeation and not Joule heating effects (7). In short, while there may be some reservations regarding the details of the analysis of permeation transients on straining electrodes, there can be no doubt that cathodically charged hydrogen enters nickel, induces serrated yielding and leads to intergranular embrittlement at depths well beyond that expected if lattice diffusion were the only active hydrogen transport mechanism.

Perhaps a more relevant issue is to determine how to separate the contributions of thermal or Joule effects from dislocation transport, in cases when both are significant transient phenomena. This effort is continuing.

In the context of the question of dislocation transport of hydrogen, Appendix A describes recent experiments performed in order to study the influence of plastic deformation on hydrogen transport in a $2\frac{1}{4}$ Cr-1Mo steel (8). In short, the results of this work suggest that dislocations act as traps for hydrogen and <u>decrease</u> the rate of transport. Such behavior, it should be noted, is in contrast to that observed in nickel-base alloys, described above, which indicates that mobile dislocations significantly increase (apparent) hydrogen diffusion rates.

Appendix B describes work which we believe provides evidence for grain boundary diffusion of hydrogen in nickel. In this case, both electrochemical hydrogen permeation techniques and Ion Microprobe Analysis were used to study grain boundary transport. This work (9) indicates that the grain boundary diffusivity was on the order of 60 times faster than lattice diffusion of hydrogen in nickel.

The required index of technical reports and index of publications are given in Appendices C and D.

References

1. R.M. Latanision, M. Kurkela, and F. Lee, in Hydrogen Effects in Metals, p. 379 (AIME, Warrendale) 1981.

2. R.M. Latanision and H. Opperhauser, Jr., Met. Trans., 5, 483 (1974).

3. R.M. Latanision and R.W. Staehle, Scripta Met., 2, 667 (1968).

4. M. Kurkela and R.M. Latanision, Scripta Met., 13, 927 (1979).

5. M. Kurkela, Sc.D. Thesis, MIT, 1981.

6. R. Otsuka and M. Isaji, Scripta Met., 15, 1153 (1981).

7. M. Kurkela and R.M. Latanision, Scripta Met., 15, 1157 (1981).

8. M. Kurkela, G.S. Frankel, R.M. Latanision, S. Suresh, and R.O. Ritchie, Scripta Met., in press

9. T. Tsuru and R.M. Latanision, Scripta Met., in press.

Appendix A

INFLUENCE OF PLASTIC DEFORMATION ON HYDROGEN
TRANSPORT IN 2 1/4 Cr-1Mo STEEL

M. Kurkela, G.S. Frankel, and R.M. Latanision
Department of Materials Science and Engineering
Massachusetts Institute of Technology
Cambridge, MA 02139

and

S. Suresh and R.O. Ritchie
Department of Materials Science and Mineral Engineering
University of California
Berkeley, CA 94720

Introduction

The role of hydrogen in influencing the fracture characteristics of metals has been a subject of detailed investigations for many years. Although the precise nature of the hydrogen embrittlement process is not clearly understood, many current theories consider the transport of hydrogen from possible external sources into the bulk of a metal or from various internal sources to critical locations as being an important step in the embrittlement mechanism.

It was first suggested by Bastien and Azou (1) that mobile dislocations carry hydrogen in the form of Cottrell atmospheres. Frank (2) reported the first experimental evidence of enhanced outgassing of hydrogen in mild steels due to plastic deformation. Tritium release (3) and slip plane decoration (4) measurements have suggested the possibility of hydrogen transport by dislocations in a number of materials. Quantitative models for dislocation-aided transport of hydrogen have been discussed by Tien et al. (5) and by Johnson and Hirth (6,7). Recent studies by Kurkela and Latanision (8,9) show that hydrogen transport associated with dislocation motion in nickel may occur at rates considerably greater than those due to lattice diffusion. On the other hand, experiments by Berkowitz and Heubaum (10) on 4130 steel undergoing simultaneous hydrogen charging and plastic deformation reveal slower hydrogen permeation rates dues to plastic strain. It has been suggested that this may be due to dislocation-enhanced trapping of hydrogen rather than transport.

The objective of this paper is to present results on the effect of plastic deformation on hydrogen transport in a 2 1/4 Cr-1Mo low strength pressure vessel steel. Hydrogen permeation experiments have been carried out over a range of strain rates using electrochemical techniques modified to allow plastic deformation. The results are interpreted to reflect trapping of hydrogen due to dislocations and the possible reasons for the differences in hydrogen transport behavior between b.c.c. ferrous and f.c.c. nickel-base alloys are discussed.

Experimental

The steel used in the present investigation is a fully bainitic 2 1/4 Cr-1Mo pressure vessel steel, ASTM A542 Class 3 (hereafter referred to as SA542-3). The chemical composition, heat treatment and ambient temperature mechanical properties of this steel are listed in Table I. The material was available in the form of a thick plate (300x175x140 mm) from which tensile specimens 1.52 and 0.76 mm in thickness were machined with a gage length of

TABLE I

i) Chemical composition (wt%)

C	Mn	Si	Ni	Cr	Mo	Cu	P	S
0.12	0.45	0.21	0.11	2.28	1.05	0.12	0.014	0.015

ii) Heat treatment

    a) Austenitize 5 1/2 hr at 954°C + water quench

    b) Temper 8 hr at 663°C

    c) Stress relieve 15 hr at 593°C
                   22 hr at 649°C
                   18 hr at 663°C

iii) Mechanical properties

Yield Strength (MPa)	U.T.S. (MPa)	Elongation (%)	Reduction in Area (%)
496	610	25	77

Charpy impact energy (J)	K_{Ic} (MPa$\sqrt{m}$)	K_{Iscc} (MPa$\sqrt{m}$)
197	295	>85

50.8 mm and reduced section width of 19.1 mm. For permeation studies, the specimens were polished with emery paper (up to 500 grit finish) and the gage section of the anodic side was coated with palladium by electroless deposition from a Pallamerse* solution.

The hydrogen permeation experiments were carried out using the electrochemical technique of Devanathan and Stachurski (11), modified to allow plastic deformation of the specimen and simultaneous charging. Details of the experimental set-up have been described elsewhere (8). The specimen was mounted between two electrochemical cells with the specimen-cell assembly positioned between the crossheads of an Instron tensile testing machine. The anodic side containing 0.1N NaOH was potentiostated at -50mV SCE while the cathodic side containing 0.1N H_2SO_4 + 10 mg $NaAsO_2$ (per liter) was galvanostatically controlled. Hydrogen charging was performed at a current density of 1.0 mA/cm^2. Specimens were deformed over a range of strain rates varying from 1.67 x 10^{-5} to 1.67 x 10^{-4} sec^{-1} and the permeation currents and load were recorded as a function of time. All experiments were performed at ambient temperatures.

Results

Fig. 1 shows the permeation transient for SA542-3 steel tested in the unstrained condition. It is found that the diffusion coefficient of hydrogen, D_H, is (5.1± 0.3) x 10^{-7} cm^2/sec and the steady state permeation flux (45.0±1.5)μA/cm^2. Both numbers are the mean values from four experiments. The magnitude of D_H obtained in the present study is in agreement with the available data for steels having a similar composition (12).

To study the effect of plastic deformation on hydrogen transport, two types of experiments were conducted. In the first case (type 1), a steady-state permeation current through the specimen was initially established without any deformation, after which the specimen was plastically deformed, with charging continued during straining. In the second case (type 2), the specimen was strained initially and once the background current (which increases initially due to deformation) stabilized, hydrogen charging was begun.

The results of an experiment of the first type (for strain rate $\dot{\varepsilon}$ = 1.67 x 10^{-5} sec^{-1})

* Trademark
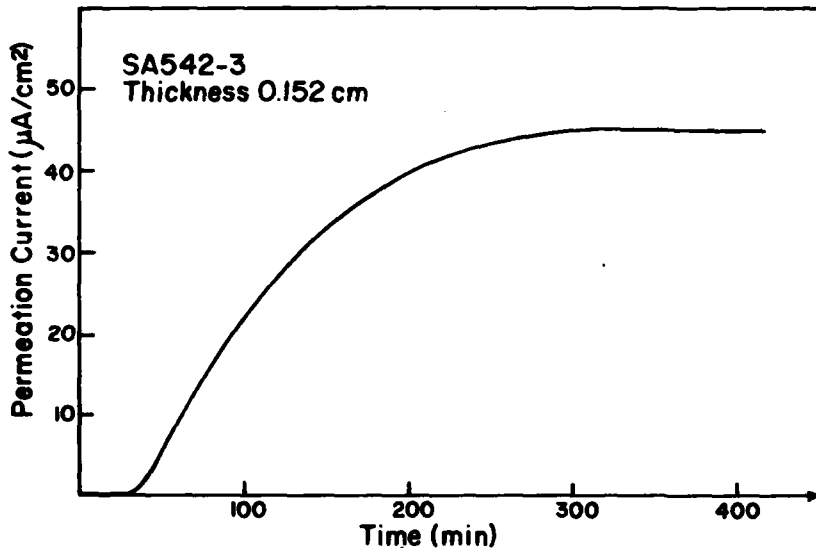
FIG. 1
Hydrogen permeation in
unstrained SA542-3.

are shown in Fig. 2. First, a steady state permeation current is established without any
applied stress. Now, as the specimen is deformed, a drastic reduction in hydrogen permeation
current is observed at the yield point. The results also indicate an inverse relationship
between the permeation flux and the flow stress (Fig. 2). This qualitatively agrees with
the findings of Berkowitz and Heubaum (10) for 4130 steel, with the decrease in hydrogen
permeation, however, being more pronounced in 2 1/4 Cr-1Mo steel.
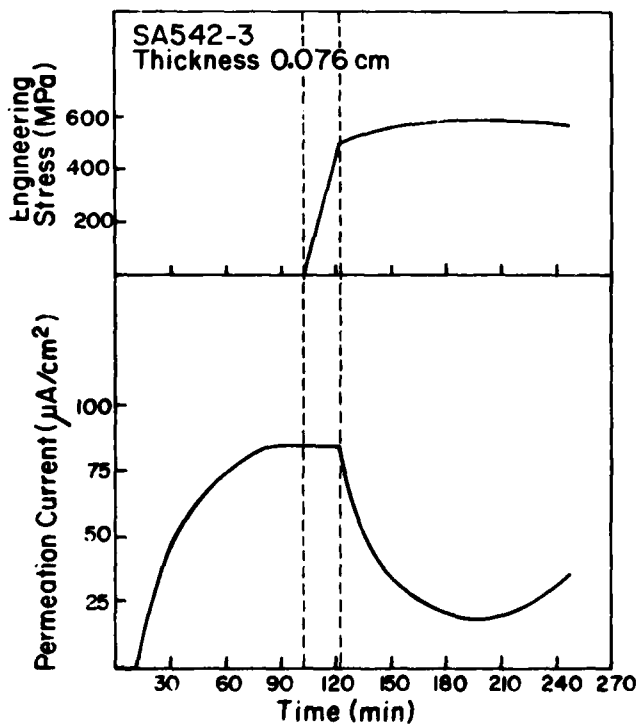
FIG. 2
Hydrogen permeation in SA542-3 during
simultaneous hydrogen charging and
plastic deformation (type 1).
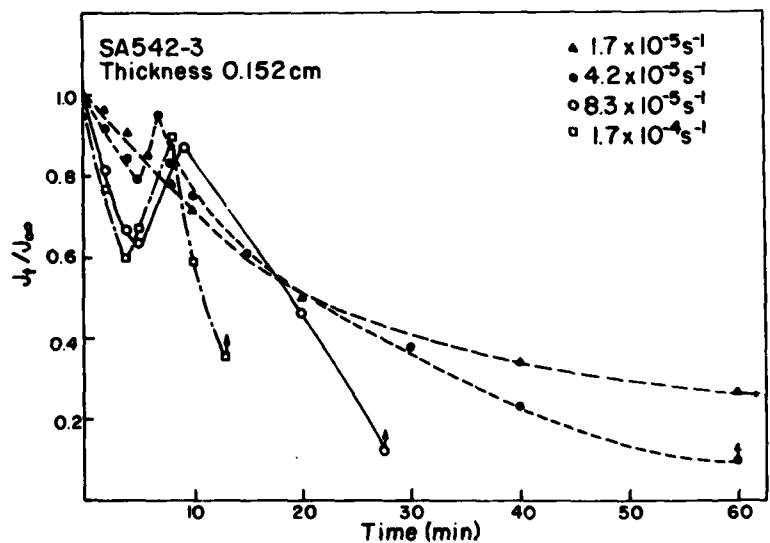
FIG. 3
Normalized permeation flux (J_t/J_∞) vs. time
plot in the plastic region of the stress-
strain curve as a function of strain rate.

The reduction in hydrogen permeation flux in the plastic region is given as a function of time in Fig. 3 for four different strain rates. The permeation flux is plotted in the normalized form, J_t/J_∞ where J_∞ is the steady-state permeation flux prior to deformation and J_t the flux at any time t. It is noted that the initial decrease in permeation flux occurs at shorter durations of plastic deformation at higher strain rates. Also, for the three highest strain rates, there is a sharp increase in permeation flux after the initial drop, the enhancement apparently being a function of strain rate. Upon reaching the peak value, the permeation current starts to decrease, the rate of decrease again being a function of the strain rate. The results of an experiment of the second type are illustrated in Fig. 4. At the onset of plastic deformation, the anodic current initially increases to reach a steady state value. At this point, *hydrogen charging is begun while deformation is continued throughout the test.* The value of diffusion coefficient D_H, calculated from the resulting permeation transient, is 2.6×10^{-7} cm^2/sec, which is about half of the value obtained before (Fig. 1) for an unstrained specimen of SA542-3. It is considered that the difference between the two values of D_H is due to the traps created by plastic straining.

Discussion

The significant drop in permeation current at the onset of plastic deformation (Figs. 2 and 3) suggests that the increase in dislocation density due to plastic strain creates traps which act as "sinks" for hydrogen and decrease the rate of hydrogen transport. The continuous decrease in hydrogen permeation during deformation seems to indicate that the rate of trap creation exceeds the rate of trap filling. An overall trend of decreasing permeation flux with plastic deformation is observed, despite the small peaks in the J_t/J_∞ versus time plots. Although the precise mechanistic reasons for the occurrence of such peaks are currently not understood, it is conceivable that such secondary effects are associated with the relative changes in the rate of trap creation (i.e., dislocation generation) and the rate of trap filling. The dependence of peak height on strain rate is consistent with such an explanation. The role of strain rate in accelerating the rate

FI . 4
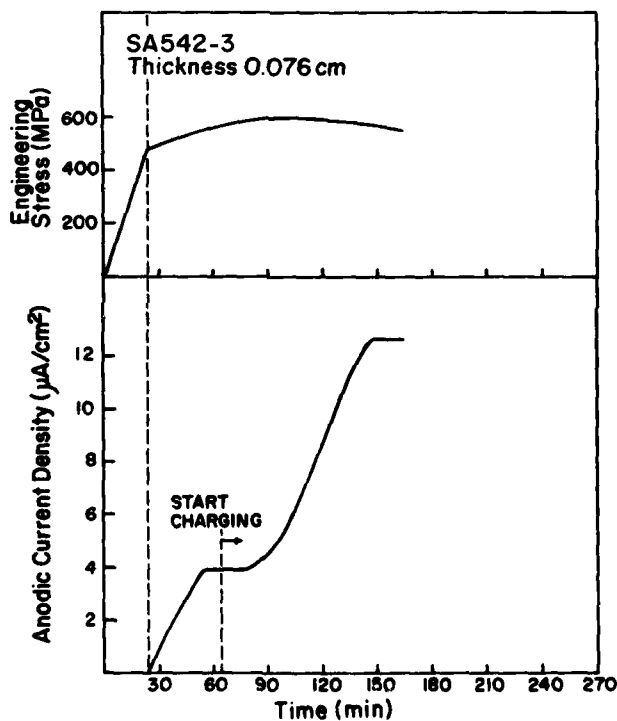
Hydrogen p ~~tio .n SA542-3 during simultaneous
charging and ast.. deformation (type 2).

of decrease of hydrogen permeation (Fig. 3) indicates that dislocations are the main trapping sites for hydrogen. The overall behavior observed for SA542-3 steel is in accordance with that reported by Berkowitz and Heubaum (10) for 4130 steel, with only the magnitude of reduction in hydrogen transport rate due to trapping being much greater for the present 2 1/4 Cr-1Mo steel.

The results of experiments in which the tensile specimen was first deformed without being charged (type 2) indicate that the effective diffusivity, in fact, decreases as a result of plastic deformation. This is contrary to the observed role of dislocations in hydrogen permeation for nickel and nickel-base alloys (8,9), where plastic deformation has been found to result in hydrogen transport several orders of magnitude faster than that in unstrained samples.

Thus, it is found that while dislocation-aided enchancements in hydrogen permeation occur in nickel-base alloys, hydrogen trapping plays a dominant role in ferrous alloys. In light of this, it is interesting to consider the works of Oriani (13) and Thomas (14) on hydrogen trapping in b.c.c. ferrous alloys and in f.c.c. nickel and stainless steels, respectively. In ferritic alloys, the binding energy of hydrogen to dislocations is several times higher than the bulk activation energy for diffusion (0.4 eV versus 0.1 eV) (13). In f.c.c. materials, such as Ni and stainless steels, the opposite effect is observed: the binding energy of hydrogen to dislocations is several times smaller than the diffusional activation energy (i.e., 0.1 eV versus 0.4-0.5 eV) (14). Moreover, the form in which hydrogen is associated with dislocations (i.e., localized core atmospheres or diffuse Cottrell atmospheres) and the interaction distance for such atmospheres may depend on the lattice structure (6) and could influence the transport rate of hydrogen.

In summary, hydrogen interactions with dislocations and other traps are strong in ferritic steels, whereas interactions in f.c.c. alloys are weak. This difference may explain why dislocations transport hydrogen in one case and trap it in the other.

Conclusions

Hydrogen permeation experiments on a 2 1/4 Cr-1Mo steel undergoing simultaneous hydrogen charging and plastic deformation indicate that dislocations act as traps for hydrogen and decrease the rate of hydrogen transport. Such reductions in hydrogen permeation are found to be inversely related to the strain rate and are more pronounced at higher strain rates. The present results are in contrast to the behavior observed in nickel-base alloys where mobile dislocations significantly accelerate hydrogen diffusion rates.

Acknowledgements

References

1. P. Bastien and P. Azou, C.R. Acad. Sci., Paris, 232, 1845 (1951).
2. R.C. Frank, in Internal Stresses and Fatigue in Metals, G.M. Rassweiler and W.L. Grube, eds., Elsevier Press, New York, 411 (1959).
3. M.R. Louthan, Jr., G.R. Caskey, Jr., J.A. Donovan, and D.E. Rawl, Jr., Mater. Sci. Eng., 10, 357, (1972).
4. L.M. Foster, T.H. Jack, and W.W. Hill, Met. Trans., 1A, 3117 (1970).
5. J.K. Tien, A.W. Thompson, I.M. Bernstein, and R.J. Richards, Met. Trans., 7A, 821 (1976).
6. H.H. Johnson and J.P. Hirth, Met. Trans., 7A, 1543 (1976).
7. J.P. Hirth and H.H. Johnson, in Proc. NATO Advanced Research Institute on Atomistics of Fracture, R.M. Latanision and J.R. Pickens, eds., Plenum Press, in press.
8. M. Kurkela and R.M. Latanision, Scripta Met., 13, 927 (1979).
9. M. Kurkela, Sc.D. Thesis, Massachusetts Institute of Technology, 1981.
10. B.J. Berkowitz and F.H. Huebaum, in Proc. NATO Advanced Research Institute on Atomistics of Fracture, R.M. Latanision and J.R. Pickens eds., Plenum Press, in press.
11. M.A. Devanathan and Z. Stachurski, Proc. Roy. Soc., A270, 90 (1962).
12. P. Wilson, M. Smialowski, and S. Smialowska, Ohio State University, private communication (1980).
13. R.A. Oriani, Acta Met., 18, 147 (1980).
14. G.J. Thomas, in Hydrogen Effects in Metals, I.M. Bernstein and A.W. Thompson, eds., The Metallurgical Society of AIME, 77 (1981).

Appendix B

GRAIN BOUNDARY TRANSPORT
OF HYDROGEN IN NICKEL

T. Tsuru and R.M. Latanision
Department of Materials Science and Engineering
Massachusetts Institute of Technology
Cambridge, MA 02139

Introduction

The intergranular, hydrogen-induced embrittlement of nickel has been widely discussed and the role of various phenomena such as solute (particularly metalloid) segregation (1), hydrogen transport by lattice diffusion as well as by mobile dislocations (2), hydrogen-induced plasticity (3), etc., has been considered. Birnbaum (4) has recently reviewed the hydrogen related fracture of metals. Grain boundary transport of hydrogen has been considered less likely and previous gas phase (5) as well as electrolytic (6) permeation measurements have failed to produce evidence of grain boundary diffusion. Recent ion microprobe (IMA) experiments suggest that hydrogen (duterium) segregation occurs at grain boundaries in Nb and Ni (4). The object of this communication is to report evidence of grain boundary diffusion of hydrogen in nickel using IMA and electrochemical methods.

Experimental

Strips of Ni 270 (99.97% Ni) were cold rolled to thickness ranging from 0.15 to 0.06 mm. After a mechanical polish, the specimens were annealed at 1050°C for 3 min and then water quenched. To induce the segregation of impurities, some specimens were aged at 600°C for 24 hr under an argon atmosphere and then water quenched. The grain diameter of these specimens was 50 to 150μm.

The method developed by Devanathan and Stachurski (7) was used for the measurement of hydrogen permeation rate. $0.1N-H_2SO_4$ and $0.1N-NaOH$ were used as catholyte and anolyte, respectively.

Initially, anodic polarization in $0.1N-NaOH$ at 0.1 V (SCE) was performed for more than 24 hr. When the anodic current decayed to less than 10 nA/cm^2 and the current transient became neglible, the catholyte was filled into the cathodic compartment of the cell and galvanostatic cathodic polarization (6.6 or 1 mA/cm^2) for hydrogen charging started immediately. Subsequent increase in anodic current was attributed to the permeation flux of hydrogen. It should be noted that Pd was not plated onto the anode surface, as is often the case, in these experiments in order to achieve low background anodic current densities (8)

For IMA measurements, the anodic side of specimen was polished with 0.3μm alumina paste and covered by a lacquer. After hydrogen charging for a certain period from the uncoated cathode side, the specimen was wrapped in aluminum foil and kept in a liquid nitrogen vessel. Just before IMA (CAMECA) analysis of the anode side, the lacquer was dissolved off in acetone. This was intended to avoid contamination and minimize the escape of hydrogen from the anodic surface.

Results and Discussion

A typical result of the electrolytic permeation measurement is shown in Fig. 1. The rmeation flux due to lattice diffusion increased over a period of several hours depending on the specimen thickness and then reached steady state after more than ten hours. In the arly stages of permeation, a very small incremental increase in the anodic or exit current
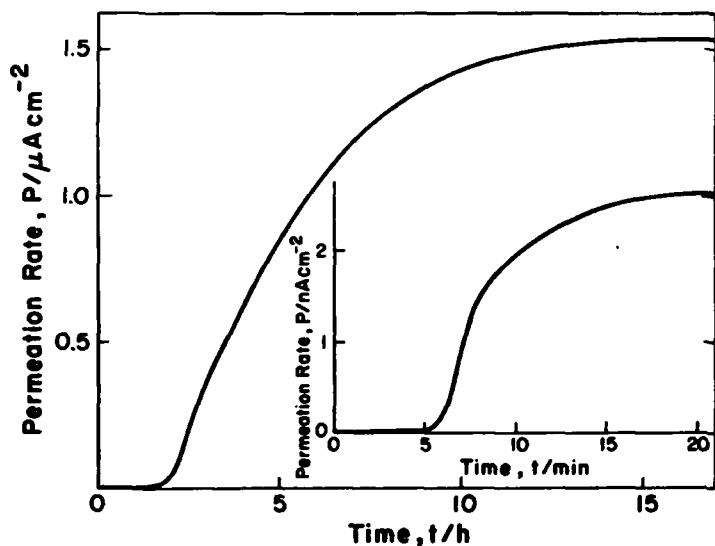
FIG. 1
Electrolytic hydrogen permeation transients
showing lattice and grain boundary (insert)
transport.
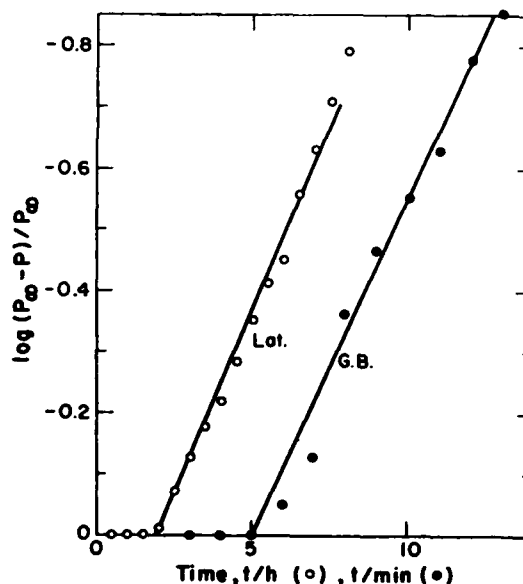
FIG. 2
Logarithmic dependence of the perme-
ation flux on time.

occurred after a few minutes and reached a steady state current within 10 to 20 min, as
shown in Fig. 1. Since this increment was a few nA/cm^2 which corresponded to about one
thousandth of the permeation flux through lattice diffusion, it was presumably buried in
the noise in some earlier measurements (6) and sensitive to the surface preparation. It
is presumed that this small transient corresponds to a grain boundary diffusion flux.
Similar observations have been made recently in gas phase charging experiments by Fidelle
(9).

The diffusion constant was calculated from the breakthrough time t_b and the lag time
t_{lag} as follows (7):

$$t_b = \frac{L^2}{15.3\,D} \quad [1] \quad \text{and} \quad t_{lag} = \frac{L^2}{6\,D} \quad [2]$$

where L is the thickness of the specimen and D is the diffusion constant. It has also been
shown (7) that the plot of log $(P_\infty - P_t)/P_\infty$ against time, for the rise transient, is a
straight line with a slope $1/t_0$, where

$$t_0 = L^2/\pi^2 D \quad [3]$$

Fig. 2 shows those plots for the lattice diffusion and the early stage of permeation which
presumably corresponds to grain boundary diffusion.

Both lattice and grain boundary diffusion constants were independent of the sample
thickness, which affected only the steady state fluxes. Similarly, the addition of a
promoter for hydrogen absorption, 3 mg/l of $NaAsO_2$, increased the steady state flux but
did not sensibly affect the diffusion constants.

The mean values and standard deviations of measured diffusion constants are given in
Table 1. The lattice diffusion constant compares well with that determined by gas phase
charging (5). The grain boundary diffusion constant was approximately 60 times (between
20 to 100) larger than that corresponding to lattice diffusion. This is not as large
differences as may be expected but may be reasonable for intestitial hydrogen. Notice in

TABLE 1
Measured Diffusion Constants

	Lattice Diffusion $D_{lat} (cm^2/sec)$	Grain Boundary Diffusion $D_{gb} (cm^2/sec)$
Annealed (1050°C)	$(3.52 \pm 1.02) \times 10^{-10}$ $\overline{n} = 11$	$(2.05 \pm 1.50) \times 10^{-8}$ $n = 5$
Annealed + Aged (Aged at 600°C/24 hr)	$(3.38 \pm 0.91) \times 10^{-10}$ $\overline{n} = 4$	$(2.13 \pm 0.93) \times 10^{-8}$ $n = 2$

n = number of independent measurements

Table 1 that both lattice and grain boundary diffusion constants were only slightly affected by thermal treatment (aging) intended to induce grain boundary segregation of sulfur. Similarly, Birnbaum (4) has observed (thermally charged) hydrogen accumulation at grain boundaries both in the presence of segregated sulfur and in its absence. It is, of course, possible that an alternate thermal treatment might give rise to the segregation of other species and to a quite different response. The influence of thermal treatment is still under study.

Since the average grain size of the specimen was around 100μm, we can roughly estimate the length of grain boundary lines as 200 cm in 1 cm^2 surface of the specimen. Assuming a grain boundary width which is effective for the rapid grain boundary diffusion as 10 Å (10), the effective area of grain boundary, S_{gb}, is considered as 2×10^{-5} cm^2 per unit surface area. So the grain boundary and lattice fluxes per unit surface area can be written as

$$i_{gb} = k\, S_{gb} D_{gb} \qquad \text{and} \qquad i_{lat} = k\, D_{lat} \qquad [4]$$

where k is a constant. Since the ratio of the diffusion constants was about 60 and the steady state flux through lattice diffusion was measured to be about 2μA/cm^2, the steady state flux through grain boundary diffusion should be around 2.4nA/cm^2. This rough estimation agrees fairly well with experimental results.

An IMA measurement was made on a specimen of 0.12 mm thickness which corresponds to a breakthrough time for the lattice and grain boundary diffusion of about 8 hr and 8 min, respectively. The specimen was charged with hydrogen for 2 hr; in short, the charging time is long enough for hydrogen to permeate the specimen by grain boundary transport but not by lattice diffusion. The result of a step scan analysis of 60_{Ni}^{+} and 1_{H}^{+} (10μm each step and 13μm resolution) is shown in Fig. 3 in which three hydrogen peaks can be seen. This suggests that there were spots where the concentration of hydrogen was very large compared with the matrix. Fig. 4 shows the sputtered surface where the IMA measurement was performed and the line of circles which corresponds to the trace of the IMA spot measurements. These peaks correspond to the points of intersection of the IMA scan direction vector with grain boundaries in the specimen as shown in Fig. 4. In essence, the concentration of hydrogen at grain boundaries was found to be very large compared to background hydrogen. Notice as well that the nickel signal is little affected in crossing grain boundaries - i.e., the ratio $1_{H}^{+}/60_{Ni}^{+}$ increases significantly. We consider these observations to be consistent with the suggestion of grain boundary diffusion that emerged from the electrolytic permeation experiments described earlier.
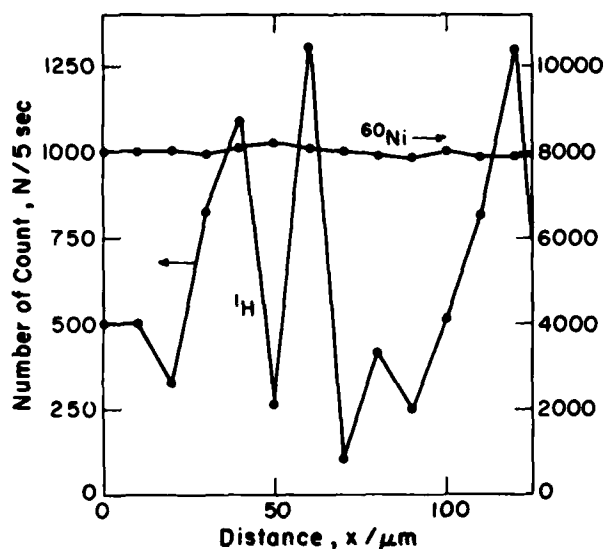
FIG. 3
IMA data showing the increased hydrogen
concentration at grain boundaries on the
exit surface of a nickel specimen cathod-
ically charged for 2 hours at the opposite
or entry surface (cathode).
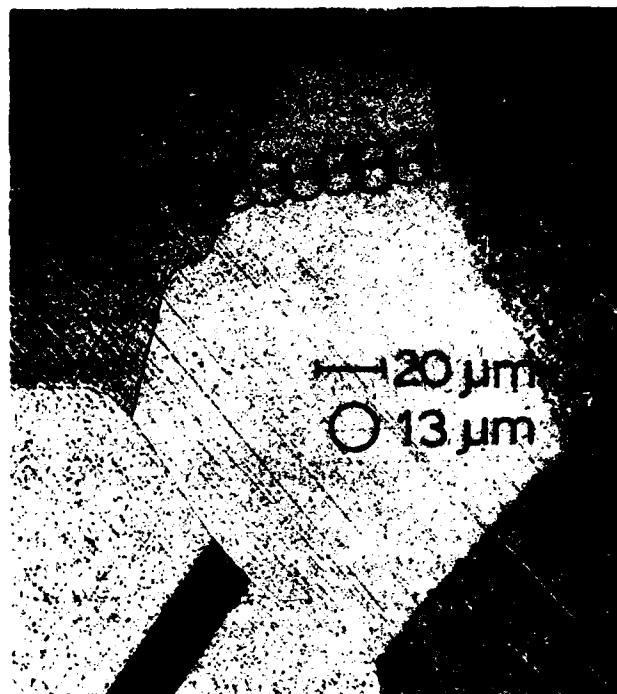
FIG. 4
IMA scanning direction superimposed on the
optical micrograph of the surface corre-
sponding to Fig. 3. The hydrogen peaks in
Fig. 3 correspond to grain boundary inter-
sections.

Conclusion

The present experiments suggest that the grain boundary diffusion constant for hydrogen
in pure nickel is larger than that for lattice diffusion. Both lattice and grain boundary
diffusion constants appear to be independent of the specimen thickness, the segregation of
sulfur and the presence of promoters of hydrogen absorption in the electrolyte. IMA
measurements are compatible with the rapid diffusion of hydrogen along grain boundaries.

Acknowledgements

References

1. R.M. Latanision, M. Kurkela and F. Lee, in Hydrogen Effects in Metals, eds., I.M.
   Bernstein and A.W. Thompson, p. 379, (TMS-AIME, Warrendale) 1981.
2. M. Kurkela and R.M. Latanision, Scripta Met., 13, 927 (1979).
3. T. Masumoto, J. Eastman and H.K. Birnbaum, Scripta Met., 15, 1033 (1981).
4. H.K. Birnbaum, in Proc. NATO Advanced Research Institute on Atomistics of Fracture,
   eds., R.M. Latanision and J.R. Pickens, (Plenum Press, NY) in press.
5. W.M. Robertson, Z. Metallkd., 64, 436 (1973).
6. M. Kurkela, Sc.D. Thesis, Massachusetts Institute of Technology, 1981.
7. M.A.V. Devanathan and Z. Stachurski, Proc. Roy. Soc., A270, 90 (1962).
8. M. Kurkela and R.M. Latanision, Scripta Met., 15, 1157 (1981).
9. J.P. Fidelle, private communication, September 1981.
10. P.G. Shewmon, Diffusion in Solids, p. 164, (McGraw-Hill, NY) 1963.

Appendix C

Technical Reports

R.M. Latanision, O.H. Gastine, and C.R. Compeau, "Stress Corrosion Cracking and Hydrogen Embrittlement: Differences and Similarities", Technical Report No. 1, January 1978.

R.M. Latanision, F.T.S. Lee, and M. Kurkela, "Hydrogen Induced Intergranular Cracking of Nickel-Base Alloys", Technical Report No. 2, October 1978.

M. Kurkela and R.M. Latanision, "The Effect of Plastic Deformation on the Transport of Hydrogen in Nickel", Technical Report No. 3, September 1979.

M. Kurkela, F.T.S. Lee, and R.M. Latanision, "Hydrogen-Induced Intergranular Cracking of Nickel-Base Alloys", Technical Report No. 4, July 1980.

R.M. Latanision, M. Kurkela, and F.T.S. Lee, "The Role of Grain Boundary Chemistry and The Environment on Intergranular Fracture", Technical Report No. 5, October 1980.

R.M. Latanision, "Atomistics of Environmentally-Induced Fracture", Technical Report No. 6, May 1981.

Appendix D

Publications

R.M. Latanision, O.H. Gastine, and C.R. Compeau, "Stress Corrosion Cracking and Hydrogen Embrittlement: Differences and Similarities", in Environment Sensitive Fracture of Engineering Materials, ed., Z.A. Foroulis, p. 48-70 (AIME, Warrendale) 1979.

M. Kurkela and R.M. Latanision, "The Effect of Plastic Deformation on the Transport of Hydrogen in Nickel", Scripta Met., 13, 927-932 (1979).

R.M. Latanision, M. Kurkela, and F.T.S. Lee, "The Role of Grain Boundary Chemistry and the Environment on Intergranular Fracture", in Hydrogen Effects in Metals, eds., I.M. Bernstein and A.W. Thompson, p. 379-395 (AIME, Warrendale) 1981.

B.J. Berkowitz, M. Kurkela, and R.M. Latanision, "The Effect of Ordering on the Hydrogen Embrittlement Susceptibility of Ni$_2$Cr", in Hydrogen Effects in Metals, eds., I.M. Bernstein and A.W. Thompson, p. 411-418 (AIME, Warrendale) 1981.

M. Kurkela and R.M. Latanision, "Concerning Electrochemical Measurements of Hydrogen Permeation in Metals", Scripta Met., 15, 1157-1161, (1981).

R.M. Latanision, "Atomistics of Environmentally-Induced Fracture", in Atomistics of Fracture, eds., R.M. Latanision and J.R. Pickens, (Plenum, NY) in press.

M. Kurkela, G.S. Frankel, R.M. Latanision, S. Suresh, and R.O. Ritchie, "Influence of Plastic Deformation on Hydrogen Transport in 2^1/4 Cr-1Mo Steel", Scripta Met., in press.

T. Tsuru and R.M. Latanision, "Grain Boundary Transport of Hydrogen in Nickel", Scripta Met., in press.

M. Kurkela and R.M. Latanision, "Hydrogen Transport by Dislocations in Nickel and Ni-Base Alloys", submitted to Met. Trans.

M. Kurkela and R.M. Latanision, "Hydrogen Permeability and Diffusivity in Ni and Ni-Base Alloys", submitted to Corrosion.

BASIC DISTRIBUTION LIST

Technical and Summary Reports   April 1978

Organization	Copies	Organization	Copies
Defense Documentation Center Cameron Station Alexandria, VA 22314	12	Naval Air Propulsion Test Center Trenton, NJ 08628 ATTN: Library	1
Office of Naval Research Department of the Navy 800 N. Quincy Street Arlington, VA 22217		Naval Construction Batallion Civil Engineering Laboratory Port Hueneme, CA 93043 ATTN: Materials Division	1
ATTN: Code 471 Code 102 Code 470	1 1 1	Naval Electronics Laboratory San Diego, CA 92152 ATTN: Electron Materials Sciences Division	1
Commanding Officer Office of Naval Research Branch Office Building 114, Section D 666 Summer Street Boston, MA 02210	1	Naval Missile Center Materials Consultant Code 3312-1 Point Mugu, CA 92041	1
Commanding Officer Office of Naval Research Branch Office 536 South Clark Street Chicago, IL 60605	1	Commanding Officer Naval Surface Weapons Center White Oak Laboratory Silver Spring, MD 20910 ATTN: Library	1
Office of Naval Research San Francisco Area Office 760 Market Street, Room 447. San Francisco, CA 94102	1	David W. Taylor Naval Ship Research and Development Center Materials Department Annapolis, MD. 21402	1
Naval Research Laboratory Washington, DC 20375		Naval Undersea Center San Diego, CA 92132 ATTN: Library	1
ATTN: Codes 6000 6100 6300 6400 2627	1 1 1 1 1	Naval Underwater System Center Newport, RI 02840 ATTN: Library	1
Naval Air Development Center Code 302 Warminster, PA 18964 ATTN: Mr. F. S. Williams	1	Naval Weapons Center China Lake, CA 93555 ATTN: Library	1
		Naval Postgraduate School Monterey, CA 93940 ATTN: Mechanical Engineering Department	1

.anization	Copies	Organization	Copies
Naval Air Systems Command Washington, DC 20360 ATTN: Codes 52031 52032	1	NASA Headquarters Washington, DC 20546 ATTN: Code RRM	1
Naval Sea System Command Washington, DC 20362 ATTN: Code 035	1	NASA Lewis Research Center 21000 Brookpark Road Cleveland, OH 44135 ATTN: Library	1

Naval Facilities Engineering
  Command
Alexandria, VA 22331
ATTN: Code 03
	1	National Bureau of Standards
		Washington, DC 20234
		ATTN: Metallurgy Division
		       Inorganic Materials Div.
			1
			1

Scientific Advisor Commandant of the Marine Corps Washington, DC 20380 ATTN: Code AX	1	Director Applied Physics Laboratory University of Washington 1013 Northeast Fortieth Street Seattle, WA 98105	1
Naval Ship Engineering Center Department of the Navy Washington, DC 20360 ATTN: Code 6101	1	Defense Metals and Ceramics Information Center Battelle Memorial Institute 505 King Avenue Columbus, OH 43201	1
Army Research Office P.O. Box 12211 Triangle Park, NC 27709 ATTN: Metallurgy & Ceramics Program	1	Metals and Ceramics Division Oak Ridge National Laboratory P.O. Box X Oak Ridge, TN 37380	1
Army Materials and Mechanics Research Center Watertown, MA 02172 ATTN: Research Programs Office	1	Los Alamos Scientific Laboratory P.O. Box 1663 Los Alamos, NM 87544 ATTN: Report Librarian	1

Air Force Office of Scientific
  Research
Bldg. 410
Bolling Air Force Base
Washington, DC 20332
ATTN: Chemical Science Directorate
      Electronics & Solid State
       Sciences Directorate
	1
	1
		Argonne National Laboratory
		Metallurgy Division
		P.O. Box 229
		Lemont, IL 60439
			1

Air Force Materials Laboratory Wright-Patterson AFB Dayton, OH 45433	1	Brookhaven National Laboratory Technical Information Division Upton, Long Island New York 11973 ATTN: Research Library	1
Library Building 50, Rm 134 Lawrence Radiation Laboratory Berkeley, CA	1	Office of Naval Research Branch Office 1030 East Green Street Pasadena, CA 91106	1

SUPPLEMENTARY DISTRIBUTION LIST

Technical and Summary Reports

Dr. T. R. Beck
Electrochemical Technology Corporation
10035 31st Avenue, NE
Seattle, Washington 98125

Professor I. M. Bernstein
Carnegie-Mellon University
Schenley Park
Pittsburgh, Pennsylvania 15213

Professor H. K. Birnbaum
University of Illinois
Department of Metallurgy
Urbana, Illinois 61801

Dr. Otto Buck
Rockwell International
1049 Camino Dos Rios
P. O. Box 1085
Thousand Oaks, California 91360

Dr. David L. Davidson
Southwest Research Institute
8500 Culebra Road
P. O. Drawer 28510
San Antonio, Texas 78284

Dr. D. J. Duquette
Department of Metallurgical Engineering
Rensselaer Polytechnic Institute
Troy, New York 12181

Professor R. T. Foley
The American University
Department of Chemistry
Washington, D. C. 20016

Mr. G. A. Gehring
Ocean City Research Corporation
Tennessee Avenue & Beach Thorofare
Ocean City, New Jersey 08226

Dr. J. A. S. Green
Martin Marietta Corporation
1450 South Rolling Road
Baltimore, Maryland 21227

Professor R. H. Heidersbach
University of Rhode Island
Department of Ocean Engineering
Kingston, Rhode Island 02881

Professor H. Herman
State University of New York
Material Sciences Division
Stony Brook, New York 11970

Professor J. P. Hirth
Ohio State University
Metallurgical Engineering
1314 Kinnear Road
Columbus, Ohio 43212

Dr. E. W. Johnson
Westinghouse Electric Corporation
Research and Development Center
1310 Beulah Road
Pittsburgh, Pennsylvania 15235

Professor R. M. Latanision
Massachusetts Institute of Technology
77 Massachusetts Avenue
Room E19-702
Cambridge, Massachusetts 02139

Dr. F. Mansfeld
Rockwell International Science Center
1049 Camino Dos Rios
P. O. Box 1085
Thousand Oaks, California 91360

Dr. Jeff Perkins
Naval Postgraduate School
Monterey, California 93940

C
January 1979

SUPPLEMENTARY DISTRIBUTION LIST
(Continued)

Professor H. W. Pickering
Pennsylvania State University
Department of Material Sciences
University Park, Pennsylvania 16802

Dr. E. A. Starke, Jr.
Georgia Institute of Technology
School of Chemical Engineering
Atlanta, Georgia 30332

Dr. Barry C. Syrett
Stanford Research Institute
333 Ravenswood Avenue
Menlo Park, California 94025

Dr. R. P. Wei
Lehigh University
Institute for Fracture and
  Solid Mechanics
Bethlehem, Pennsylvania 18015

Professor H. G. F. Wilsdorf
University of Virginia
Department of Materials Science
Charlottesville, Virginia 22903

Dr. Clive Clayton
State University of New York
Material Sciences Division
Stony Brook, New York 11970